Electronic Spectra of 2,2′-Bithiophene and 2,2′:5′,2″-Terthiophene Radical Cations: A Theoretical Analysis

Mercedes Rubio,[†] Enrique Ortí,[‡] Rosendo Pou-Amérigo,[§] and Manuela Merchán*

Departamento de Química Física, Instituto de Ciencia Molecular, Universitat de València, Dr. Moliner 50, Burjassot, E-46100 Valencia, Spain

Received: May 14, 2001; In Final Form: July 31, 2001

Analysis of the electronic spectra of 2,2′-bithiophene and 2,2′:5′,2″-terthiophene radical cations has been performed by using multiconfigurational second-order perturbation theory (CASPT2). Atomic natural orbital (ANO) type basis sets of split valence quality, including polarization functions on all heavy atoms, have been used. In agreement with experimental data, in the energy range below the lowest optically allowed transition of the respective neutral system, theoretical results predict two main absorption bands for both cations. The 2^2A_u and 3^2A_u states computed at 1.94 and 2.80 eV, respectively, are related to the corresponding band maxima recorded for bithiophene cation. The 1^2B_1 state of terthiophene cation placed at 1.31 eV is assigned to the observed lowest-energy band. Nevertheless, according to the present results, the highest-energy band observed in terthiophene cation stems from two electronic transitions. They involve the 2^2B_1(1.94 eV) and 3^2B_1(2.12 eV) excited states.

1. Introduction

Polythiophenes and oligothiophenes are among the most investigated conjugated polymers and oligomers. They have many interesting technological applications. Oligothiophenes are used, for instance, as active components in optoelectronic devices such as light-emitting diodes,[1] field-effect transistors,[2] and photovoltaic cells.[3] The reasons for the spectacular development of these compounds are related to their good environmental stability, in both neutral and doped states, and to their structural versatility which has led to the synthesis of a large number of substituted derivatives as a way of improving and controlling the electrical and optical properties.[4−6]

The most promising applications of conjugated polymers and oligomers are currently based on neutral systems. Nevertheless, the initial interest in conjugated polymers arose from the observed pronounced increase in the electrical conductivity upon doping, i.e., after oxidation or reduction.[7] The increase of electrical conductivity is attributed to the generation of localized charged defects associated with structural distortions along the polymer chains as a consequence of the oxidation or reduction process.[8] Such charged defects are considered to be the charge carriers in the conduction mechanism. For polymers with a nondegenerate ground-state structure, like polythiophenes, only the so-called polaron and bipolaron defects are possible.[8] From a chemical point of view, polarons and bipolarons are related to radical ions and spinless divalent ions, respectively. The electronic structure of conjugated polymers is therefore expected to undergo important modifications upon doping due to the presence of charged defects. Electronic spectroscopy has significantly contributed to reveal such electronic structure changes. It has been widely used for identifying the type of charged defects formed in the polymer chains at different doping levels, in combination with electron spin resonance (ESR) spectroscopy. On the basis of one-electron band structure models,[8] three and two electronic transitions at intragap energies have been traditionally ascribed to polarons and bipolarons, respectively. Nevertheless, from spectroscopic studies on radical ions and divalent ions of oligomers, the spectroscopic signatures of polarons and bipolarons have been subsequently reassigned.[9,10]

The current research has focused on the radical cations of the shortest α-oligothiophenes, 2,2′-bithiophene and 2,2′:5′,2″-terthiophene (hereafter called bithiophene and terthiophene, respectively). Charged oligothiophenes have been the subject of many spectroscopic studies.[11−23] Most of them have been performed on substituted oligothiophenes because of the inherent reactivity of the short-chain radical cations, having a marked trend to polymerize,[18,19] and the low solubility of the long-chain compounds.

As far as we know, the chemical oxidation of unsubstituted α-oligothiophenes was first performed by Fichou et al.[18,19] These studies included oligomers containing from three to six thiophene rings and used $FeCl_3$ as oxidant in highly dilute dichloromethane solutions to prevent aggregation between oligomers. The cationic species formed were subsequently characterized by means of electronic absorption and ESR spectroscopies. Two intense bands were observed in the absorption spectra of the radical cations flanked with sidebands of weaker intensity at higher energies. Fichou et al. assigned each of the four reported bands to a different electronic transition on the basis of the transitions expected for a polaron defect according to band structure models. Because of the high reactivity of the radical cation of terthiophene, its absorption spectrum could not be, however, recorded in those experimental conditions.[18,19] Transient absorption spectroscopy made possible to measure the absorption spectra of the radical cations of bithiophene and terthiophene, which were photochemically generated in the presence of electron acceptors.[20] Wintgens et al.[22] extended the study to the radical cations of quaterthiophene and sexithiophene. The

---

* Corresponding author. Manuela.Merchan@uv.es. Phone: +34 96-398-3155. FAX: +34 96-398-3156.

[†] Mercedes.Rubio@uv.es.

[‡] Enrique.Orti@uv.es.

[§] Rosendo.Pou@uv.es.

10.1021/jp011824l CCC: $20.00

absorption spectra of the short-chain photogenerated radical cations show one strong band in the visible region of the spectrum and a less intense band at lower energies. For the long-chain oligomers, the latter appears out of the experimental energy range examined.[20,22] No sidebands are recorded on the upper energy side of the two observed bands, in contrast to the features found in the absorption spectra of chemically prepared oligothiophene radical cations.[18,19] The band maxima appear at similar energies independently of how the radical cations are generated.[18−20,22] As expected, both bands shift to lower energies as the size of the oligomer increases. The radical cations of oligothiophenes, from thiophene to sexithiophene, have been recently produced by pulse radiolysis in dichloromethane and their UV−vis spectra characterized.[23]

The interpretation of the absorption spectra of charged oligothiophenes is further complicated by the dimerization process observed in radical cations.[11−15] They tend to reversibly form π-dimers in solution at high concentrations or low temperatures, being the dimerization more favored as the size of the oligomer increases.[14,15] Such π-dimers have been spectroscopically detected by the appearance of two new bands on the upper energy side of the absorption bands observed for the radical cation. A third band related to an intermolecular charge-transfer transition emerges at low energies.

Less attention has been paid to the spectroscopic properties of oligothiophene ions from the theoretical point of view. As far as we know, only the 2,2′-bithiophene radical cation has been recently studied at the ab initio level by means of CASSCF linear response methodology.[24] In addition, two semiempirical studies have been reported on oligomers of increasing size, making it possible to analyze the evolution of the properties with the chain length.[25,26] The computed excitation energies on these studies are, however, quite sensitive to the semiempirical method used. As discussed elsewhere, a similar situation occurs for neutral bithiophene[27] and terthiophene.[28]

In the present contribution, we are mainly concerned with the low-lying excited states of the radical cations of bithiophene and terthiophene in order to clarify the spectroscopic characteristics of charge-induced polaron defects. A structural characterization of such defects is also provided. The study has been carried out using the complete active space CAS(SCF) method[29] in combination with a second-order perturbation approach, the CASPT2 method.[30,31] The successful performance of the CASPT2 method in computing differential correlation effects for excitation energies has been illustrated in a number of earlier applications.[32−34] Particularly relevant for this work are the studies on the electronic spectra of bithiophene,[27] terthiophene,[28] biphenyl,[35] and biphenyl radical cation and anion.[36] Our previous researches on the spectroscopic properties of these systems have provided a detailed interpretation of their spectra. In particular, the studies involving biphenyl have made it possible to rationalize the evolution of the electronic structure of the system upon doping. The results obtained for the excited states of bithiophene and terthiophene radical cations are presented here. Reliable assignments are given for the electronic spectra of both radical cations.

2. Details of Calculations

Planar structures have been assumed for the ground state of the radical cations of bithiophene and terthiophene. The cis and trans isomers have been calculated for bithiophene cation in order to analyze the influence of the cis−trans isomerism on the structural and spectroscopic properties of these systems. Experimental studies have shown the existence of this isomerism for oligothiophene radical ions, and the trans orientation has been found for bithiophene to be energetically favored.[37,38] For the terthiophene radical cation, the study has concentrated on the all-trans planar isomer.

To determine the influence of the method on the structural parameters, full geometry optimizations of *trans*-bithiophene cation were performed at different calculation levels within C_{2h} symmetry. In particular, the MP2, CASSCF, and DFT methods were used in combination with the 6-31G* basis set and the Dunning's correlation-consistent cc-pVDZ basis set. As discussed in next section, the UB3-PW91/cc-pVDZ calculation level was finally adopted to optimize the ground-state structures of the three systems studied, that is, *s-cis-* and *s-trans-*bithiophene and *all-trans*-terthiophene radical cations.

Generally contracted basis sets of atomic natural orbital (ANO) type have been used throughout the spectroscopic study. They have been built from S(17s12p5d)/C(14s9p4d)/H(8s) primitive sets[39,40] using the same contraction scheme S[4s3p1d]/C[3s2p1d]/H[2s] as that in previous studies on bithiophene and terthiophene neutral molecules.[27,28] The basis set was shown to describe the excited states with enough flexibility to achieve the required accuracy at a moderate computational cost.

The low-lying excited states of bithiophene and terthiophene cations have been computed by means of the complete active space second-order perturbation theory (CASPT2).[30,31] In this method, the reference wave function and the molecular orbitals are determined using the CASSCF approximation.[29] The average CASSCF procedure has been used to compute the states of a given symmetry. The corresponding ground states, however, were obtained from a single-root calculation. For the systems considered, the 1s-core orbitals were kept frozen in the form determined by the corresponding ground-state Hartree−Fock (HF) wave function, and the σ valence electrons and the sulfur 2s and 2p electrons were inactive. All electrons except the cores were included in the CASPT2 calculation, at the second-order level of the correlation energy treatment.

The π-valence active space, comprising 10 orbitals with 11 active electrons, has been used in the calculations of both *s-trans-* and *s-cis*-bithiophene cations. The equivalent active space for terthiophene cation comprises 15 active orbitals and 17 electrons, a size still too large for the present implementation of the software. As in the previous study of the neutral molecule,[28] the three deepest π-orbitals have been treated as inactive, which results in a 12 orbitals/11 electrons active space. The level-shift technique (LS-CASPT2)[41,42] was used to remove certain intruder states involving the deepest π-orbitals. To determine the lowest value of the level-shift parameter which provides stable excitation energies for all computed states, calibration calculations were carried out with the level-shift parameter within the energy range 0.2−0.4 au. A value of 0.3 au was used for the LS-CASPT2 calculations performed for the terthiophene cation. The effect of extending the active space on the computed excitation energies was also examined for a few states. As expected, the extension of the active space to 14 orbitals/15 electrons led to excitation energies similar to those provided by the level-shift technique but at an extremely high computational cost.

The oscillator strengths were evaluated following the usual procedure:[32] transition moments computed at the CASSCF level, by means of the CASSCF state interaction (CASSI) method,[43] and excitation energies obtained at the CASPT2 level.

The CASSCF/CASPT2 and CASSI calculations were carried out with the MOLCAS-4 quantum chemistry software.[44] The

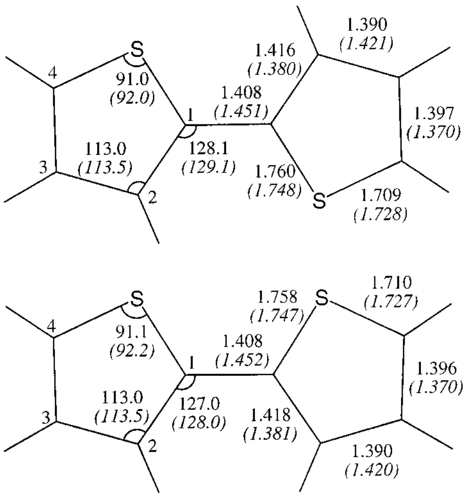

Figure 1. Geometries optimized at the UB3-PW91/cc-pVDZ level for the ground state of *s-trans-* and *s-cis*-bithiophene radical cations. The geometries calculated for the ground state of the neutral molecules are given within parentheses. Bond lengths are in Å and bond angles in deg.

DFT package of the GAUSSIAN 94 program[45] was used for the geometry optimizations.

3. Results and Discussion

The results and discussion are organized as follows. The equilibrium geometries of the ground state of bithiophene and terthiophene radical cations are first analyzed. The results for the low-lying excited states of both cations are subsequently considered and compared to the corresponding available experimental data.

3.1. Ground-State Geometry Determinations. The geometry of the ground-state *trans*-bithiophene cation was first optimized within C_{2h} symmetry constraints at different calculation levels. Since MP2/6-31G* optimized geometries were used for the neutral molecules in our previous spectroscopic studies,[27,28] the UMP2/6-31G* level was chosen as starting approach. However, the calculated structural parameters were rejected because of the large spin contamination obtained at the UMP2/6-31G* level. The CASSCF method and the density functional theory (DFT), using the cc-pVDZ basis set, were next applied to optimize the corresponding geometries. The π-valence active space (10 active orbitals/11 active electrons) was used in the CASSCF calculation. The hybrid B3−PW91 functional[46,47] was chosen for the DFT calculation on the basis of the results obtained in a study performed by Viruela et al. on 2,2′-bithiophene.[48]

The geometries predicted for bithiophene cation at the UB3−PW91/cc-pVDZ and π-CASSCF/cc-pVDZ levels are very similar. The C−C bond distances and bond angles differ by less than 0.007 Å and 1.0°, respectively. The C_1-S bond distance (see Figure 1 for atom numbering), however is computed to be 0.02 Å longer at the UB3−PW91/cc-pVDZ level (1.760 Å) than at the π-CASSCF/cc-pVDZ level (1.741 Å), consistent with previous findings reported by Keszthelyi et al.[24] These authors have suggested that the CASSCF value is more accurate. To determine the relative accuracy of those results, optimization of the C_1-S bond distance at the CASPT2/cc-pVDZ level was carried out by using a pointwise procedure, with the remaining structural parameters fixed at their optimal π-CASSCF/cc-pVDZ values. The optimized C_1-S bond distance at the CASPT2 level was computed to be 1.756 Å, close to the optimal UB3−PW91/cc-pVDZ value. In light of these results, the UB3−PW91/cc-pVDZ calculation level was used in the present study to optimize the ground-state structures of all the systems investigated.

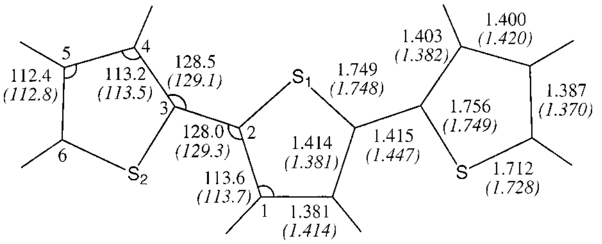

Figure 2. Geometry optimized at the UB3-PW91/cc-pVDZ level for the ground state of planar *all-trans*-terthiophene radical cation. The geometry calculated for the ground state of the neutral molecule is given within parentheses. Bond lengths are in Å and bond angles in deg.

Planar or nearly planar geometries are expected for both bithiophene and terthiophene cations from simple molecular orbital considerations. The highest occupied molecular orbital (HOMO) is antibonding with respect to the inter-ring bonds. These bonds are therefore strengthened upon ionization, thus preventing internal rotation. Hence, only planar structures have been considered. The geometries of the ground states have been fully optimized within C_{2h} symmetry for *s-trans*-bithiophene cation and within C_{2v} symmetry for *s-cis*-bithiophene and *all-trans*-terthiophene cations. The ground state of the cation belongs to the ^2B_g ($^2A_2$) irreducible representations within C_{2h} (C_{2v}) point groups. The computed UB3−PW91/cc-pVDZ equilibrium geometries for bithiophene and terthiophene cations are depicted in Figures 1 and 2, respectively. For the sake of comparison, the structural parameters obtained for the neutral molecules at the B3−PW91/cc-pVDZ level are also included in Figures.

As Figure 1 shows, there is a strong similarity between the s-cis and s-trans structures of bithiophene cation, the bond lengths of both conformers differing at most by 0.002 Å. A distortion toward a quinoid structure is produced upon ionization and is characterized by the reversal of the sequence of long and short C−C bonds on going from the neutral to the oxidized form. The C_1-C_1' and C_2-C_3 bonds shorten and the C_1-C_2 and C_3-C_4 bonds lengthen. The inter-ring (C_1-C_1') bond distance has the most important change, and it acquires a double-bond character. Differences about 0.03 Å are found for the remaining C−C bond distances, the changes for the C−S bond distances being smaller. Bond angles are affected by less than 1.0° upon ionization.

A similar quinoid distortion is determined for the *all-trans*-terthiophene cation (see Figure 2). The structural distortion extends over the whole molecule, but the changes tend to diminish on going to the most external C−C bonds. Thus, the central ring has a larger bond length alternation. As for the bithiophene cation, the most affected bond lengths upon ionization are the inter-ring distances, which are shortened by 0.03 Å. The X-ray crystal structures of a substituted terthiophene (3′,4′-dibutyl-5,5″-diphenyl-2,2′:5′,2″-terthiophene) and of its hexafluorophosphate salt have been reported.[49] The comparison of both structures supports the quinoid-type distortion predicted here for terthiophene cation. In general, the geometries of many organic oligomers have been predicted to evolve from an aromatic-type structure to a quinoid-type structure upon charging (see, for instance, ref 36 and references cited therein).

3.2. Excited States of Bithiophene Radical Cation. The ground and excited states of bithiophene cation arising from excitations within the π-orbital manifold belong to the B_g and

TABLE 1: Principal Configurations and Weights and Number and (Weights) of Singly, Doubly, and Triply Excited Configurations[a] with Coefficients Larger than 0.05 for the Ground and Lowest Doublet Excited States of Bithiophene Radical Cation

		weight			
state	principal configurations	(%)	S	D	T
	s-trans Isomer				
$1^2\mathrm{B}_g$	$(3\mathrm{a}_u)^2(3\mathrm{b}_g)^2(4\mathrm{a}_u)^2(4\mathrm{b}_g)^1$	84	4 (3%)	9 (4%)	–
$1^2\mathrm{A}_u$	$(3\mathrm{a}_u)^2(3\mathrm{b}_g)^2(4\mathrm{a}_u)^1(4\mathrm{b}_g)^2$	63	11 (81%)	9 (5%)	1 (<1%)
	$(3\mathrm{a}_u)^2(3\mathrm{b}_g)^2(4\mathrm{a}_u)^2(5\mathrm{a}_u)^1$	9			
$2^2\mathrm{B}_g$	$(3\mathrm{a}_u)^2(3\mathrm{b}_g)^1(4\mathrm{a}_u)^2(4\mathrm{b}_g)^2$	75	7 (81%)	8 (4%)	2 (1%)
$2^2\mathrm{A}_u$	$(3\mathrm{a}_u)^1(3\mathrm{b}_g)^2(4\mathrm{a}_u)^2(4\mathrm{b}_g)^2$	54	9 (82%)	9 (4%)	–
	$(3\mathrm{a}_u)^2(3\mathrm{b}_g)^2(4\mathrm{a}_u)^2(5\mathrm{a}_u)^1$	18			
	$(3\mathrm{a}_u)^2(3\mathrm{b}_g)^2(4\mathrm{a}_u)^1(4\mathrm{b}_g)^2$	7			
$3^2\mathrm{A}_u$	$(3\mathrm{a}_u)^2(3\mathrm{b}_g)^2(4\mathrm{a}_u)^2(5\mathrm{a}_u)^1$	44	14 (78%)	11 (7%)	–
	$(3\mathrm{a}_u)^1(3\mathrm{b}_g)^2(4\mathrm{a}_u)^2(4\mathrm{b}_g)^2$	18			
	$(3\mathrm{a}_u)^2(3\mathrm{b}_g)^2(4\mathrm{a}_u)^1(4\mathrm{b}_g)^2$	5			
	s-cis Isomer				
$1^2\mathrm{A}_2$	$(3\mathrm{b}_1)^2(4\mathrm{b}_1)^2(3\mathrm{a}_2)^2(4\mathrm{a}_2)^1$	84	3 (3%)	9 (3%)	–
$2^2\mathrm{A}_2$	$(3\mathrm{b}_1)^2(4\mathrm{b}_1)^2(3\mathrm{a}_2)^1(4\mathrm{a}_2)^2$	76	6 (80%)	13 (6%)	4 (1%)
$1^2\mathrm{B}_1$	$(3\mathrm{b}_1)^2(4\mathrm{b}_1)^1(3\mathrm{a}_2)^2(4\mathrm{a}_2)^2$	51	12 (81%)	10 (5%)	1 (<1%)
	$(3\mathrm{b}_1)^2(4\mathrm{b}_1)^2(3\mathrm{a}_2)^2(5\mathrm{b}_1)^1$	18			
$2^2\mathrm{B}_1$	$(3\mathrm{b}_1)^1(4\mathrm{b}_1)^2(3\mathrm{a}_2)^2(4\mathrm{a}_2)^2$	55	12 (82%)	12 (4%)	1 (<1%)
	$(3\mathrm{b}_1)^2(4\mathrm{b}_1)^1(3\mathrm{a}_2)^2(4\mathrm{a}_2)^2$	13			
	$(3\mathrm{b}_1)^2(4\mathrm{b}_1)^2(3\mathrm{a}_2)^2(5\mathrm{b}_1)^1$	9			
$3^2\mathrm{B}_1$	$(3\mathrm{b}_1)^2(4\mathrm{b}_1)^2(3\mathrm{a}_2)^2(5\mathrm{b}_1)^1$	42	14 (77%)	16 (9%)	–
	$(3\mathrm{b}_1)^1(4\mathrm{b}_1)^2(3\mathrm{a}_2)^2(4\mathrm{a}_2)^2$	13			
	$(3\mathrm{b}_1)^2(4\mathrm{b}_1)^1(3\mathrm{a}_2)^2(4\mathrm{a}_2)^2$	7			
	$(3\mathrm{b}_1)^1(4\mathrm{b}_1)^2(3\mathrm{a}_2)^2(4\mathrm{a}_2)^1(5\mathrm{b}_1)^1$	6			

[a] With respect to the ground-state principal configuration.

TABLE 2: CASPT2 Vertical Excitation Energies (Δ*E*, in eV) and Oscillator Strengths (*f*) for the Lowest Excited States of the Radical Cation of Bithiophene and Available Experimental Data (Exp)

s-trans			*s*-cis			
state	Δ*E*	f^a	state	Δ*E*	f^a	exp
$1^2\mathrm{B}_g$			$1^2\mathrm{A}_2$			
$1^2\mathrm{A}_u$	1.54	0.010 (51°)	$2^2\mathrm{A}_2$	1.56	0.003 (S)	
$2^2\mathrm{B}_g$	1.78	forbidden	$1^2\mathrm{B}_1$	1.78	<0.001 (L)	
$2^2\mathrm{A}_u$	1.95	0.062 (12°)	$2^2\mathrm{B}_1$	1.94	0.068 (L)	2.10,[b] 2.14[c]
$3^2\mathrm{A}_u$	2.78	0.607 (18°)	$3^2\mathrm{B}_1$	2.80	0.512 (L)	2.92,[b,d] 2.95[c]

[a] Direction of the transition dipole moment with respect to the long molecular axis is given within parentheses. L and S stand for the long and short molecular axes, respectively. [b] Electronic absorption spectrum in Freon glass at 77 K.[24,53] [c] Electronic absorption spectrum in acetonitrile.[20] [d] Electronic absorption spectrum of bithiophene cation generated by pulse radiolysis in dichloromethane.[23]

A_u irreducible representations of the C_{2h} symmetry group for the s-trans isomer (molecule placed in the *xy* plane) and to the B_1 and A_2 symmetries of the C_{2v} point group for the s-cis isomer (molecule placed in the *yz* plane). The four lowest doublet excited states, three of A_u (B_1) and one of B_g (A_2) symmetries, have been considered for the s-trans (s-cis isomer). The calculated states cover the energy range up to 4.0 eV, that is, the energy region of the spectrum below the first absorption band of the neutral molecule (see ref 27 and references therein). All the states have been computed using the optimized UB3−PW91/cc-pVDZ geometries depicted in Figure 1. The main characteristics of the CASSCF wave functions for the ground and excited states are collected in Table 1. The vertical excitation energies computed at the CASPT2 level for the s-trans and s-cis bithiophene cations are listed in Table 2, together with the calculated oscillator strengths and relevant experimental information.

The results included in Table 2 confirm the characterization of the $1^2\mathrm{B}_g$ and $1^2\mathrm{A}_2$ states as the ground states of the s-trans and s-cis isomers, respectively. As could be expected from the HF molecular orbital energies calculated for the neutral molecule,[27] both states are mainly described by the electronic configuration arising from removing one electron of the HOMO orbital, which has a weight of 84% in the CASSCF wave function (see Table 1). The CASPT2 calculations predict the s-trans isomer of bithiophene cation to be 0.40 kcal/mol (∼0.02 eV) lower in energy than the s-cis isomer, in line with recent theoretical results.[24,50] From computer simulations of the experimental EPR spectrum of bithiophene cation, the two isomers, trans and cis, have been estimated to be in a ratio of about 3:2,[38] in accordance with the greater stability predicted for the trans isomer. Because of the strengthening of the inter-ring bond, interconversion of the s-trans and s-cis isomers is expected to be highly unlikely. Indeed, the rotational barrier to isomerization has been estimated to be very much higher than that of the neutral compound.[24,37,38] The vertical and adiabatic ionization potentials have been computed using as reference the minimum-energy MP2/6-31G* s-trans−gauche structure reported for neutral bithiophene by Ortí et al.[51] The vertical ionization potential is computed to be 7.58 eV at the CASPT2 level, somewhat below the gas-phase datum of 7.95 eV.[52] The computed adiabatic values are 7.21 and 7.23 eV for the s-trans and s-cis isomers, respectively.

As Table 2 shows, there is a great similarity between the electronic spectra computed for the s-trans and s-cis bithiophene cations. The computed excitation energies differ at most by 0.02 eV, and the electronic transitions are predicted to have intensities on the same order of magnitude for both isomers. There are, however, differences between the polarization of the transitions as a result of the different symmetry of the isomers. For the s-cis cation, the transitions to the $^2\mathrm{A}_2$ and $^2\mathrm{B}_1$ states are optically allowed and polarized along the short and long molecular axes, respectively. For the s-trans isomer, the $1^2\mathrm{B}_g \rightarrow {}^2\mathrm{A}_u$ electronic transitions are polarized in the molecular plane. Transitions polarized along the short and long molecular axes are thus not perfectly separated in the s-trans cation, unlike the electronic transitions of the s-cis isomer. Nevertheless, the computed transition dipole moment of the two electronic transitions predicted with the highest intensity for the s-trans cation has a small angle with the long molecular axis (12° and 18°, respectively), in line with the long-axis polarization calculated for the respective transitions of the s-cis isomer. The nature of the states involved in these transitions, as determined from the CASSCF wave functions, is also found to be quite similar for both isomers (see Table 1). We shall next focus the discussion on the results obtained for the s-trans isomer, which has been characterized to be the most stable and to exist in a larger proportion.[38] According to our results, the presence of the s-cis isomer leads to minor changes in the electronic spectrum.

The two lowest excited states of bithiophene cation are the $1^2\mathrm{A}_u$ and $2^2\mathrm{B}_g$ states and appear close in energy. The $1^2\mathrm{A}_u$ state is located at 1.54 eV above the ground state, and the corresponding electronic transition is predicted to have a low oscillator strength of 0.010. The dipole transition moment is computed to form an angle of 51° with the long molecular axis. The $2^2\mathrm{B}_g$ state, computed at 1.78 eV, is related to a dipole-forbidden electronic transition. As far as we know, these two low-lying states have not been detected experimentally. As shown in Table 1, the CASSCF wave functions of the $1^2\mathrm{A}_u$ and $2^2\mathrm{B}_g$ states are dominated by the singly excited HOMO-1($4\mathrm{a}_u$) → HOMO($4\mathrm{b}_g$) and HOMO-2($3\mathrm{b}_g$) → HOMO($4\mathrm{b}_g$) configurations, respectively. Here the HOMO orbital corre-

TABLE 3: Main Configurations and Weight of the CASSCF Wave Function, Computed Vertical Excitation Energies (eV), and Related Oscillator Strengths (*f*) for the Considered Electronic Transitions of the Radical Cation of Terthiophene

state	main configuration	weight	CASSCF	LS-CASPT2[a]	f	exp[b]
1^2A_2	$...(4a_2)^2(6b_1)^2(7b_1)^2(5a_2)^1$	79				
1^2B_1	$7b_1 \rightarrow 5a_2$	47	1.89	1.31	0.051	1.46
	$5a_2 \rightarrow 8b_1$	24				
2^2B_1	$5a_2 \rightarrow 8b_1$	28	2.91	1.94	0.643	2.25
	$7b_1 \rightarrow 5a_2$	23				
	$6b_1 \rightarrow 5a_2$	14				
3^2B_1	$6b_1 \rightarrow 5a_2$	51	3.33	2.12	0.351	
	$5a_2 \rightarrow 8b_1$	16				
2^2A_2	$4a_2 \rightarrow 5a_2$	63	3.38	2.21	0.002	
3^2A_2	$3a_2 \rightarrow 5a_2$	38	3.08	2.50	<0.001	
	$5a_2 \rightarrow 6a_2$	19				
	$7b_1 \rightarrow 8b_1$	16				

[a] Calculations at the UB3-PW91 optimized geometry for the planar all-trans isomer. A value of 0.3 au has been used for the LS parameter. [b] Experimental data from the electronic absorption spectrum in acetonitrile.[22]

sponds to that of the neutral molecule, which is half-filled in the ground state of the cation.

Indirect experimental information about the 1^2A_u and 2^2B_g states can be derived from the gas-phase photoelectron spectrum of bithiophene.[52] In this spectrum, the second and third ionization peaks, corresponding to the formation of bithiophene cation in its lowest and second excited states, are located 1.21 and 1.40 eV above the first ionization peak. These energies are not directly comparable with the computed excitation energies (1.54 and 1.78 eV) because photoelectron energies correspond to vertical ionizations from the twisted geometry of the neutral molecule, while the absorption spectrum is calculated for the planar geometry of the ground state of the cation. The ground and excited states of the cation were therefore recalculated using the minimum-energy MP2/6-31G* s-trans−gauche structure (θ = 142.24°) reported for neutral bithiophene. The 1^2A_u and 2^2B_g states appear 1.20 and 1.25 eV above the twisted ground state, in accordance with the photoelectron data.

The electronic absorption spectrum of bithiophene radical cation generated photochemically in acetonitrile solution shows two structureless bands: a strong band with maximum absorption at 420 nm (2.95 eV) and a weak band centered at 580 nm (2.14 eV).[20] The strongest band exhibits a well-resolved vibrational structure involving a progression of 680 cm^{-1} in the absorption spectrum of the cation formed by γ-irradiation of bithiophene in a Freon matrix at 77 K.[24,53] In these experimental conditions, the lowest-energy peak of the UV band appears at 425 nm (2.92 eV) with the highest intensity.[24,53] The CASPT2 calculations locate the 2^2A_u and 3^2A_u states at 1.95 and 2.78 eV, respectively. The $1^2B_g \rightarrow 3^2A_u$ transition is predicted to be approximately 10 times more intense than the excitation to the 2^2A_u state. The transition dipole moment is computed to be almost parallel to the long molecular axis for both transitions (see Table 2). The assignment of these ^2A_u states to the two experimentally observed bands is therefore clear, considering the computed excitation energies and relative intensities. Keszthelyi et al.[24] have suggested the same assignment on the basis of their linear response CASSCF results. As can be seen in Table 1, the CASSCF wave functions computed for the 2^2A_u and 3^2A_u states are mainly described by a mixing of the two singly excited HOMO-3 ($3a_u$) → HOMO ($4b_g$) and HOMO ($4b_g$) → LUMO ($5a_u$) configurations.

Emmi et al.[23] have recently generated the radical cations of oligothiophenes by pulse radiolysis in dichloromethane and measured the UV−vis spectra. Although the recorded spectrum for bithiophene cation shows two intense bands in the 500−350 nm energy region, only the lowest energy peak at 425 nm has been attributed to bithiophene cation in accordance with previous results.[20,24,53] The second peak at 350 nm (3.5 eV) has been related to a different radical species or to a triplet state of bithiophene.[23,54] The present results support this suggestion since preliminary calculations estimated the next optically allowed transition at energies higher than 4.0 eV. The 3^2B_g state calculated at 3.6 eV is indeed the only state that appears in the energy range 3.0−4.0 eV but is dipole forbidden.

Finally, it is interesting to note the correspondence between the excited states of bithiophene radical cation and the four lowest excited states characterized for biphenyl radical cation[36] regarding both the nature of the states and the relative intensities predicted for the respective electronic transitions. As for bithiophene cation, the two lowest excited states of biphenyl cation appear close in energy (1.08 and 1.26 eV). They have not been experimentally observed and involve the HOMO-1 → HOMO and HOMO-2 → HOMO excitations, respectively. The next two excited states calculated at 1.88 and 3.21 eV, with a relative intensity ratio of 1:7, give rise to the two observed absorption bands. They are mainly described by a linear combination of the HOMO-3 → HOMO and HOMO → LUMO singly excited configurations.

3.3. Excited States of Terthiophene Radical Cation. The results obtained for the ground and lowest doublet excited states of terthiophene cation are summarized in Table 3. As discussed in section 2, a level-shift parameter with a value of 0.3 au has been used in the CASPT2 calculations in order to remove the intruder states appearing in certain cases. All the calculations have been performed at the optimized UB3−PW91 geometry for the planar all-trans isomer illustrated in Figure 2. The vertical absorption spectrum computed for the cation covers the energy range up to 2.8 eV, i.e., the energy region below the lowest optically allowed transition of the neutral molecule (see ref 28 and references therein). Accordingly, six states of A_2 and B_1 symmetries involving electronic transitions of π-character have been characterized.

As expected from the HF molecular orbital energies of the neutral,[28] the 1^2A_2 state, which is mainly described by the electronic configuration with a hole in the HOMO ($5a_2$) orbital, is characterized as the ground state of the cation. The values 7.04 and 6.67 eV have been obtained for the vertical and adiabatic ionization potentials, respectively, at the CASPT2 level. Both energies are referred to the ground state of terthiophene computed at the twisted minimum-energy structure optimized at the MP2/6-31G* level with C_s symmetry. This structure is slightly more stable than the fully planar C_{2v} structure by 0.27 kcal/mol at the CASPT2 level. The computed vertical and adiabatic ionization potentials of terthiophene are lower than those predicted for bithiophene, in agreement with the decrease of the oxidation potential determined experimentally when the chain length of the oligothiophene increases.[55] As for bithiophene, the vertical ionization energy computed for terthiophene underestimates the experimental gas-phase value (7.43 eV)[52] by 0.4 eV.

The electronic spectrum of terthiophene cation photochemically formed has a very intense and broad band with absorption maximum at 550 nm (2.25 eV) and a second less intense band located at 850 nm (1.46 eV).[22] The UV−vis region of the spectrum has been recently investigated by Emmi et al.[23] for radical cations of increasing size generated by pulse radiolysis in dichloromethane. For the terthiophene cation, a prominent band is observed approximately in the range 600−480 nm (2.1−2.6 eV), with the maximum absorption wavelength peaking at 545 nm, as it occurs in the spectra previously reported.[20,22]

As can be seen in Table 3, the three lowest doublet excited states of terthiophene cation correspond to states of B_1 symmetry, which give rise to optically allowed transitions from the 1^2A_2 ground-state polarized along the long molecular axis. The 1^2B_1 state is computed at 1.31 eV above the ground state, with an oscillator strength of 0.051 for the corresponding transition. According to these results, the lowest-energy band of the spectrum, with maximum at 1.46 eV in acetonitrile solution,[22] arises from the $1^2A_2 \rightarrow 1^2B_1$ electronic transition. The CASSCF wave function of the 1^2B_1 state is mainly characterized by the singly excited configurations HOMO-1 → HOMO and HOMO → LUMO, which contribute with weights of 47% and 24%, respectively.

The 2^2B_1 and 3^2B_1 states, calculated around 2 eV above the ground state, are related to the most intense transitions of the computed electronic spectrum. Oscillator strengths of 0.643 and 0.351 have been obtained for the transitions to these states. The computed excitation energies (1.94 and 2.12 eV for the 2^2B_1 and 3^2B_1 states, respectively) and oscillator strengths suggest that these two states give rise to the intense band with maximum at 2.25 eV observed in the absorption spectrum.[20,22,23] This assignment is consistent with the broadness and shape of the experimental band since it shows a shoulder on the high energy side, in agreement with the relative values of the computed oscillator strengths for the 2^2B_1 and 3^2B_1 states and the computed energy difference between them. As far as we know, this is the first time that the observed band is attributed to two electronic transitions. The pronounced multiconfigurational character of the corresponding CASSCF wave functions, in particular for the 2^2B_1 state, is remarkable.

The next excited states are the 2^2A_2 and 3^2A_2 states computed at 2.21 and 2.50 eV, respectively. These states appear close in energy to the intense $^2B_1$ states and are also in the energy range where the prominent absorption band is detected.[23] Transitions from the ground state to the $^2A_2$ states are dipole allowed and polarized along the short molecular axis. As shown in Table 3, a relatively low intensity is, however, predicted for both transitions. These two $^2A_2$ states are therefore expected to be hidden at the high-energy side of the intense peak at 2.25 eV.[20,22,23]

3.4. Final Discussion. In addition to their intrinsic interest, bithiophene and terthiophene radical cations can be considered as models of the shortest positive polaron defects which can be formed in doped polythiophenes. As stated in the Introduction, polaron defects, as well as other charged defects in conjugated polymers, have been usually identified by means of electronic spectroscopy, in particular by the presence of transitions at intragap energies. For both oligothiophene cations, we have examined the energy region of the electronic spectrum situated below the first absorption band of the neutral oligomer in order to achieve a better understanding of the changes which can be expected in the absorption spectrum due to the formation of radical cations.

The lowest singlet excited state for *s-trans*-bithiophene, the 1^1B_u state, was computed at 3.88 eV and was found to have a large multiconfigurational character dominated by the HOMO → LUMO singly excited configuration (43% of the weight in the CASSCF wave function).[27] A lower excitation energy of 2.86 eV was obtained for the 1^1B_2 state of terthiophene, characterized as the lowest singlet excited state and found to be mainly described by the HOMO → LUMO excitation (76% of the CASSCF wave function).[28] As discussed in the previous papers,[27,28] these states account for the lowest energy band observed in the electronic spectra of the neutral molecules, and the computed excitation energies are in good agreement with the experimental data. For bithiophene, the second singlet excited state (2^1B_u) was predicted to appear at 4.15 eV close in energy to the 1^1B_u state and was also suggested to contribute to the experimental band.[27] Calculations on bithiophene cation predict three dipole-allowed doublet excited states related to electronic transitions with energies lower than that of the 1^1B_u state of the neutral molecule. Five doublet excited states are found for terthiophene cation below 2.8 eV. As a whole, the states calculated are characterized by one-electron promotions from the highest doubly occupied π-molecular orbitals to the half-filled HOMO orbital and by the HOMO → LUMO excitation.

In the energy range studied (see Table 2 and Table 3), two and three detectable transitions are predicted for bithiophene and terthiophene cations, respectively, As discussed above, such transitions result in the appearance of two absorption bands for both cations at energies lower than those of the neutral oligomer, in accordance with the experimental data.[12,20,22] Spectroscopic studies on longer oligothiophenes also observe two absorption bands for radical cations at intragap energies, which shift to lower energies as the chain length increases.[14−16,18,19] However, our results reveal that the highest energy band in terthiophene cation stems from two electronic transitions involving the 2^2B_1 and 3^2B_1 states. In contrast, one state is responsible for each band in bithiophene cation. Similarly to bithiophene cation, two electronic states have been characterized and assigned to the observed bands in longer oligothiophene radical cations on the basis of the results obtained from theoretical studies at the semiempirical level.[25,26] At this point, the question of whether more than two excited states are responsible for the two observed bands in the electronic spectra of longer oligothiophene cations can be raised. Just the formulation of such a possibility can be considered as a remarkable conclusion derived from the present research. It is worth mentioning that the suggestion is consistent with the shape and broadness of the experimental bands.[23] Of course, to provide a definitive answer, high-level theoretical results should have also to be carried out for longer oligothiophene radical cations.

4. Summary

The present results provide a structural characterization of the bithiophene and terthiophene radical cations, as well as a detailed interpretation of their electronic spectra. A geometry relaxation toward a more quinoid structure in comparison with that of the neutral molecule has been determined for both cations. In addition, the computed excitation energies are in agreement with the available experimental data. On the other hand, bithiophene and terthiophene radical cations represent models for "isolated" polaron defects in doped polythiophenes. The present results have also been examined from this point of view. According to our results, a polaron defect in polythiophenes is expected to be spectroscopically characterized by two absorption bands at intragap energies, as also indicated by the experimental evidence on longer oligothiophene radical cations.[14−16,18,19] However, two electronic transitions have been found to be responsible for the high-energy band of terthiophene radical cation.

Acknowledgment. The research reported in this contribution has been supported by the European Commission through the TMR Network Contract ERB FMRX-CT96-0079 (Quantum Chemistry for the Excited State), the Projects PB97-1377 and PB98-1447 of the Spanish DGES-MEC, and the *Generalitat Valenciana*.

References and Notes

(1) Geiger, F.; Stoldt, M.; Schweizer, H.; Bäuerle, P.; Umbach, E. *Adv. Mater.* **1993**, *5*, 922.

(2) Ostoja, P.; Guerri, S.; Rossini, S.; Servidori, M.; Taliani, C.; Zamboni, R. *Synth. Met.* **1993**, *54*, 447.

(3) Noma, N.; Tsuzuki, T.; Shirota, Y. *Adv. Mater.* **1995**, *7*, 647.

(4) Fichou, D., Ed. *Handbook of Oligo- and Polythiophenes*; Wiley-VCH: Weinheim, Germany, 1999.

(5) Roncali, J. *Chem. Rev.* **1992**, *92*, 711.

(6) Roncali, J. *Chem. Rev.* **1997**, *97*, 173.

(7) Skotheim, T. A., Elsenbaumer, R., Reynolds, J. R., Eds. In *Handbook of Conducting Polymers*; Marcel Dekker: New York, 1998.

(8) Brédas, J. L.; Street, G. B. *Acc. Chem. Res.* **1985**, *18*, 309.

(9) Furukawa, Y. *Synth. Met.* **1995**, *69*, 629.

(10) Furukawa, Y. *J. Phys. Chem.* **1996**, *100*, 15644.

(11) Hill, M. G.; Mann, K. R.; Miller, L. L.; Penneau, J.-F. *J. Am. Chem. Soc.* **1992**, *114*, 2728.

(12) Hill, M. G.; Penneau, J.-F.; Zinger, B.; Mann, K. R.; Miller, L. L. *Chem. Mater.* **1992**, *4*, 1106.

(13) Zinger, B.; Mann, K. R.; Hill, M. G.; Miller, L. L. *Chem. Mater.* **1992**, *4*, 1113.

(14) Bäuerle, P.; Segelbacher, U.; Maier, A.; Mehring, M. *J. Am. Chem. Soc.* **1993**, *115*, 10217.

(15) Yu, Y.; Gunic, E.; Zinger, B.; Miller, L. L. *J. Am. Chem. Soc.* **1996**, *118*, 1013.

(16) Hotta, S.; Waragai, K. *J. Phys. Chem.* **1993**, *97*, 7427.

(17) Horowitz, G.; Yassar, A.; von Bardeleben, H. J. *Synth. Met.* **1994**, *62*, 245.

(18) Fichou, D.; Horowitz, G.; Garnier, F. *Synth. Met.* **1990**, *39*, 125.

(19) Fichou, D.; Horowitz, G.; Xu, B.; Garnier, F. *Synth. Met.* **1990**, *39*, 243.

(20) Evans, C. H.; Scaiano, J. *J. Am. Chem. Soc.* **1990**, *112*, 2694.

(21) Caspar, J. V.; Ramamurthy, V.; Corbin, D. R. *J. Am. Chem. Soc.* **1991**, *113*, 600.

(22) Wintgens, V.; Valat, P.; Garnier, F. *J. Phys. Chem.* **1994**, *98*, 228.

(23) Emmi, S. S.; D'Angelantonio, M.; Beggiato, G.; Poggi, G.; Geri, A.; Pietropaolo, D.; Zotti, G. *Radiat. Phys. Chem.* **1999**, *54*, 263.

(24) Keszthelyi, T.; Grage, M. M.-L.; Offersgaard, J. F.; Wilbrandt, R.; Svendsen, C.; Mortensen, O. S.; Pedersen, J. K.; Jensen, H. J. A. *J. Phys. Chem. A* **2000**, *104*, 2808.

(25) Cornil, J.; Beljonne, D.; Brédas, J. L. *J. Chem. Phys.* **1995**, *103*, 842.

(26) Maud, J. M. *Synth. Met.* **1999**, *101*, 575.

(27) Rubio, M.; Merchán, M.; Ortí, E.; Roos, B. O. *J. Chem. Phys.* **1995**, *102*, 3580.

(28) Rubio, M.; Merchán, M.; Ortí, E.; Roos, B. O. *Chem. Phys. Lett.* **1996**, *248*, 321.

(29) Roos, B. O. In *Advances in Chemical Physics; Ab Initio Methods in Quantum Chemistry - II*; Lawley, K. P., Ed.; Wiley: Chichester, England, 1987; Chapter 69, p 399.

(30) Andersson, K.; Malmqvist, P.-Å.; Roos, B. O.; Sadlej, A. J.; Wolinski, K. *J. Phys. Chem.* **1990**, *94*, 5483.

(31) Andersson, K.; Malmqvist, P.-Å.; Roos, B. O. *J. Chem. Phys.* **1992**, *96*, 1218.

(32) Roos, B. O.; Fülscher, M. P.; Malmqvist, P.-Å.; Merchán, M.; Serrano-Andrés, L. In *Quantum Mechanical Electronic Structure Calculations with Chemical Accuracy*; Langhoff, S. R., Ed.; Kluwer Academic Publishers: Dordrecht, The Netherlands, 1995; p 357.

(33) Roos, B. O.; Andersson, K.; Fülscher, M. P.; Malmqvist, P.-Å.; Serrano-Andrés, L.; Pierloot, K.; Merchán, M. In *Advances in Chemical Physics: New Methods in Computational Quantum Mechanics*; Prigogine, I., Rice, S. A., Eds.; Wiley: New York, 1996; Vol. XCIII:219.

(34) Merchán, M.; Serrano-Andrés, L.; Fülscher, M. P.; Roos, B. O. in *Recent Advances in Multireference Methods*; Hirao, K., Ed.; World Scientific: Singapore, 1999; Vol. IV, p 161.

(35) Rubio, M.; Merchán, M.; Ortí, E.; Roos, B. O. *Chem. Phys. Lett.* **1995**, *234*, 373.

(36) Rubio, M.; Merchán, M.; Ortí, E.; Roos, B. O. *J. Phys. Chem.* **1995**, *99*, 14980.

(37) Alberti, A.; Favaretto, L.; Seconi, G.; Pedulli, G. F. *J. Chem. Soc., Perkin Trans. 2* **1990**, p 931.

(38) Kirste, B.; Tian, P.; Kossmehl, G.; Engelmann, G.; Jugelt, W. *Magn. Reson. Chem.* **1995**, *33*, 70.

(39) Widmark, P.-O.; Malmqvist, P.-Å.; Roos, B. O. *Theor. Chim. Acta* **1990**, *77*, 291.

(40) Widmark, P.-O.; Persson, B. J.; Roos, B. O. *Theor. Chim. Acta* **1991**, *79*, 419.

(41) Roos, B. O.; Andersson, K. *Chem. Phys. Lett.* **1995**, *245*, 215.

(42) Roos, B. O.; Andersson, K.; Fülscher, M. P.; Serrano-Andrés, L.; Pierloot, K.; Merchán, M.; Molina, V. *J. Mol. Struct. (THEOCHEM)* **1996**, *388*, 257.

(43) Malmqvist, P.-Å.; Roos, B. O. *Chem. Phys. Lett.* **1989**, *155*, 189.

(44) Andersson, K.; Blomberg, M. R. A.; Fülscher, M. P.; Karlstöm, G.; Lindh, R.; Malmqvist, P.-Å.; Neogrády, P.; Olsen, J.; Roos, B. O.; Sadlej, A. J.; Schütz, M.; Seijo, L.; Serrano-Andrés, L.; Siegbahn, P. E. M.; Widmark, P.-O. *MOLCAS Version 4.0*; University of Lund: Lund, Sweden, 1997.

(45) Frisch, M. J.; Trucks, G. W.; Schlegel, H. B.; Gill, P. M. W.; Johnson, B. G.; Robb, M. A.; Cheeseman, J. R.; Keith, T.; Petersson, G. A.; Montgomery, J. A.; Raghavachari, K.; Al-Laham, M. A.; Zakrzewski, V. G.; Ortiz, J. V.; Foresman, J. B.; Cioslowski, J.; Stefanov, B. B.; Nanayakkara, A.; Challacombe, M.; Peng, C. Y.; Ayala, P. Y.; Chen, W.; Wong, M. W.; Andres, J. L.; Replogle, E. S.; Gomperts, R.; Martin, R. L.; Fox, D. J.; Binkley, J. S.; Defrees, D. J.; Baker, J.; Stewart, J. P.; Head-Gordon, M.; Gonzalez, C.; Pople, J. A. *Gaussian 94*; Gaussian, Inc.: Pittsburgh, PA, 1995.

(46) Becke, A. D. *J. Chem. Phys.* **1993**, *98*, 1372.

(47) Perdew, J. P.; Wang, Y. *Phys. Rev. B* **1992**, *45*, 13244.

(48) Viruela, P. M.; Viruela, R.; Ortí, E. *Int. J. Quantum Chem.* **1998**, *70*, 303.

(49) Graf, D. D.; Duan, R. G.; Campbell, J. P.; Miller, L. L.; Mann, K. R. *J. Am. Chem. Soc.* **1997**, *119*, 5888.

(50) Grage, M. M.-L.; Keszthelyi, T.; Offersgaard, J. F.; Wilbrandt, R. *Chem. Phys. Lett.* **1998**, *282*, 171.

(51) Ortí, E.; Viruela, P.; Sánchez-Marín, J.; Tomás, F. *J. Phys. Chem.* **1995**, *99*, 4955.

(52) Jones, D.; Guerra, M.; Favaretto, L.; Modelli, A.; Fabrizio, M.; Distefano, G. *J. Phys. Chem.* **1990**, *94*, 5761.

(53) Keszthelyi, T.; Grage, M. M.-L.; Wilbrandt, R.; Svendsen, C.; Mortensen, O. S. *Laser Chem.* **1999**, *19*, 393.

(54) Emmi, S. S.; D'Angelantonio, M.; Poggi, G.; Beggiato, G.; Camaioni, N.; Geri, A.; Martelli, A.; Pietropaolo, D.; Zotti, G. *Res. Chem. Intermed.* **1998**, *24*, 1.

(55) Xu, Z.-G.; Horowitz, G. *J. Electroanal. Chem.* **1992**, *335*, 123.